CHALMERS

FINITE ELEMENT CENTER

A finite element method on composite grids based on Nitsche's method
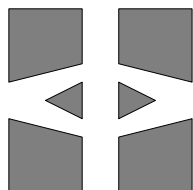
Anita Hansbo, Peter Hansbo, and Mats G. Larson

CHALMERS FINITE ELEMENT CENTER

Preprint 2002–16

A finite element method on composite grids based on Nitsche's method

Anita Hansbo, Peter Hansbo, and Mats G. Larson

CHALMERS

A finite element method on composite grids based on Nitsche's method
Anita Hansbo, Peter Hansbo, and Mats G. Larson
NO 2002–16
ISSN 1404–4382

A FINITE ELEMENT METHOD ON COMPOSITE GRIDS BASED ON NITSCHE'S METHOD

ANITA HANSBO, PETER HANSBO, AND MATS G. LARSON

ABSTRACT. In this paper we propose a finite element method for the approximation of second order elliptic problems on composite grids. The method is based on continuous piecewise polynomial approximation on each grid and weak enforcement of the proper continuity at an artificial interface defined by edges (or faces) of one the grids. We prove optimal order a priori and energy type a posteriori error estimates in 2 and 3 space dimensions, and present some numerical examples.

1. INTRODUCTION

Composite overlapping grids are commonly used with finite difference and difference-related finite volume methods, e.g., as a tool for local mesh refinement [5]. In finite element and related finite volume methods, which are inherently unstructured and thus allow for local mesh refinement, the need for overlapping mesh methods is less obvious. However, a general finite element/volume methodology for handling overlapping meshes would be a useful tool to deal with the often complicated mesh generation problem. Examples of specific applications include: (a) construction of a global mesh for a complex geometry by using overlapping meshes of elementary parts; (b) coupling of unstructured and structured meshes; and (c) coupling of boundary fitted meshes to structured or unstructured meshes, see Fig. 1.

The purpose of this paper is to introduce and analyze such a method for a model second order elliptic problem in 2 and 3 space dimensions. Unlike composite grid methods where interpolation is performed on the boundary of the overlap, cf. [2, 5], our approach is based on weak enforcement of the proper continuity across an artificial interface defined by edges (faces) of one of the meshes. The weak enforcement proposed here is constructed in such a way that the resulting scheme is stable and 'arbitrary order consistent' in the sense the exact solution satisfies the discrete equation. Hence we are able to prove optimal a priori error estimates for arbitrary order of polynomial approximation under weak mesh conditions; in particular the meshes may overlap in quite an arbitrary fashion.

FIGURE 1. Overlapping mesh FEM may be used to couple a boundary fitted mesh to an unstructured mesh (top), or to construct a global mesh by using overlapping meshes of elementary parts (bottom).

In composite grid methods, the solution on the overlap is usually computed on both (all) meshes, either using interpolation on all (artificial) interfaces [5], or by integration of products of test functions living on both meshes, as in the finite element method proposed by Brezzi, Lions, and Pironneau [4]. In contrast, in our method one only computes the solution on *one* of the meshes on the overlap; in fact, we do not require the meshes to overlap at all even though this is the situation we have in mind.

Our method stems from the work of Nitsche [10], where a method for consistent weak enforcement of Dirichlet boundary conditions was introduced, and is related, in particular, to Becker, Hansbo & Stenberg [1], where the meshes were assumed to be non-matching on the interface but shape regular on both sides of this interface. Here this last condition is relaxed, which, e.g., makes possible to use highly structured meshes in irregularly shaped subdomains. Related work includes also the mixed penalty approach analyzed in Lazarov & al. [8, 9].

An outline of the paper is as follows: In Section 2 we formulate the second order elliptic model problem and in Section 3 we state the mesh assumptions and define the numerical method used for the approximation. In Section 4.1–4.2 we demonstrate the stability of the method and derive the approximation properties of its (non-standard) finite element spaces. Optimal order a priori error estimates in a discrete energy norm, as well as in L_2-norm, are shown in Section 4.3. Our a priori analysis is in parts akin to Hansbo & Hansbo [7], where optimal order convergence was shown for a method where a material discontinuity interface was allowed to cut through the elements in an arbitrary fashion. Using similar lines of arguments as in [7], a posteriori error estimates for the control of linear functionals of the error may be derived for the present method. In this work we instead focus our attention in Section 5 on two variants of residual based a posteriori energy norm error estimates, where the element indicators of the second one are designed for ease of implementation, reducing the complications due to the geometry of the mesh. These estimates do not presuppose the saturation assumption used in [1]. Finally, in Section 6, we discuss some implementation details and present numerical examples, including a convergence study using quadratic elements i 2D as well as examples using the a posteriori error estimates as a basis for the implementation of an adaptive algorithm.

2. Problem Formulation and Preliminaries

As a model problem, we consider Poisson's equation in a bounded domain Ω in $\mathbb{R}^n$, $n = 2$ or $n = 3$, with, for simplicity, a convex polygonal boundary $\partial\Omega$. Find $u : \Omega \to \mathbf{R}$ such that

$$(2.1) \qquad -\Delta u = f \quad \text{in } \Omega,$$

$$(2.2) \qquad u = 0 \quad \text{on } \partial\Omega,$$

with $f \in L^2(\Omega)$.

Consider two given triangulations T_i^h, $i = 1, 2$, where h is a mesh size parameter. Assume that they together cover Ω, so that $\overline{\Omega} = \overline{\Omega}_1^* \cup \overline{\Omega}_2^*$ where $\overline{\Omega}_i^* = \cup_{K \in T_i^h} \overline{K}$. The meshes may overlap in an arbitrary fashion; further assumptions are given below. We then choose an (artificial) internal interface Γ composed of edges from the triangles in T_1^h and dividing Ω into two open disjoint sets Ω_i, $i = 1, 2$, such that $\Omega_i \subset \Omega_i^*$ and $\Omega = \Omega_1 \cup \Omega_2 \cup \Gamma$. We assume that the interface Γ does not depend on h, by, i.e., assuming that the mesh family T_1^h is obtained by refinement from a single coarse mesh, or by remeshing of a region Ω_1 defined from a selected mesh.

For any sufficiently regular function u in $\Omega_1 \cup \Omega_2$ we define the jump of u on Γ by $[u] := u_1|_\Gamma - u_2|_\Gamma$, where $u_i = u|_{\Omega_i}$ is the restriction of u to Ω_i. Conversely, for u_i defined in Ω_i we identify the pair $\{u_1, u_2\}$ with the function u which equals u_i on Ω_i.

Our model problem may now, due to the (artificial) interface, be written as:

$$(2.3) \qquad\qquad -\Delta u = f \quad \text{in } \Omega_1 \cup \Omega_2,$$

$$(2.4) \qquad\qquad u = 0 \quad \text{on } \partial\Omega,$$

$$(2.5) \qquad\qquad [u] = 0 \quad \text{on } \partial\Omega,$$

$$(2.6) \qquad\qquad [\nabla_{\boldsymbol{n}} u] = 0 \quad \text{on } \partial\Omega.$$

Here $\boldsymbol{n}$ denotes the exterior unit normal to Ω_1 and $\nabla_{\boldsymbol{n}} v = \boldsymbol{n} \cdot \nabla v$ is the normal flux.

For a bounded open connected domain D we shall use standard Sobolev spaces $H^r(D)$ with norm $\| \cdot \|_{r,D}$ and spaces $H_0^r(D)$ with zero trace on ∂D. The inner products in $H^0(D) = L_2(D)$ is denoted $(\cdot, \cdot)_D$. For a bounded open set $G = \cup_{i=1}^2 D_i$, where D_i are open disjoint components of G, we let $H^k(D_1 \cup D_2)$ denote the Sobolev space of functions in G such that $u|_{D_i} \in H^k(D_i)$ with norm

$$\| \cdot \|_{k,D_1 \cup D_2} = \left(\sum_{i=1}^2 \| \cdot \|_{k,D_i}^2 \right)^{1/2}.$$

3. FINITE ELEMENT SPACES AND METHOD

3.1. **The Finite Element Spaces.** We will use the following notation for mesh related quantities. Let h_K be the diameter of an element $K \in T_i^h$ and $h = \max_{K \in T_i^h, i=1,2} h_K$. To distinguish elements from the two meshes, we will sometimes use indexed element notation $K_i \in T_i^h$ for clarity.

The nodes on Γ of the elements in T_1^h, together with the points of intersection between elements in T_2^h and Γ, define a partition of Γ, $\Gamma = \cup_{j \in J_h} \overline{\Gamma^j}$. Note that each part Γ^j belongs to two elements, one from each mesh. We denote these elements by K_1^j and K_2^j, respectively. A local meshsize on Γ is defined by

$$(3.1) \qquad\qquad h(x) = h_{K_1^j}, \quad x \in \Gamma^j.$$

For any element $K \in T_i^h$, let $P_K = K \cap \Omega_i$ denote the part of K in Ω_i.

We make the following assumptions regarding the meshes:

A1: The triangulations are non-degenerate, i.e.,

$$h_K/\rho_K \leq C \quad \forall K \in T_i^h, \quad i = 1, 2,$$

where h_K is the diameter of K and ρ_K is the diameter of the largest ball contained in K.

A2: The meshes have locally compatible meshsize over Γ. More precisely, let $K_1^j \in T_1^h$ and $K_2^j \in T_2^h$ be the elements which contain a specific part Γ^j of Γ. We assume that

$$ch_{K_1^j} \leq h_{K_2^j} \leq Ch_{K_1^j} \quad \forall j \in J_h.$$

Here and below, C and c denote generic constants.

We shall seek a discrete solution $U = (U_1, U_2)$ in the space $V^h = V_1^h \times V_2^h$, where

$$V_i^h = \{\phi \in H^1(\Omega_i) : \phi|_{K \cap \Omega_i} \text{ is a polynomial of degree } p \ \forall K \in T_i^h, \ \phi|_{\partial\Omega} = 0\}.$$

Note that functions in V^h are, in general, discontinuous across Γ. As for the nodal representation of polynomials on the parts in Ω_2, see Figure 2.
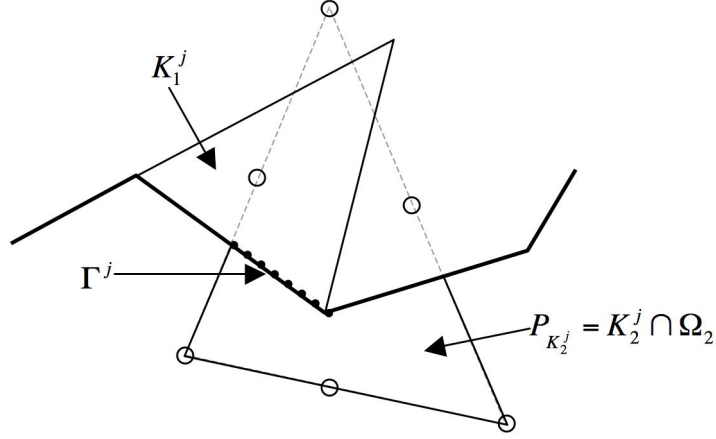

FIGURE 2. The interface Γ consists of element edges from elements in T_1^h. Each part Γ^j belongs to two triangles, $K_1^j \in T_1^h$ and $K_2^j \in T_2^h$. Nodes for representing a quadratic polynomial on the element K_2^j are indicated. The same nodes are used in the implementation to represent a polynomial on the part $P_{K_2^j} = K_2^j \cap \Omega_2$.

3.2. **The Finite Element Method.** The method is defined by the variational problem: find $U \in V^h$ such that

(3.2) $$a^h(U, \phi) = l(\phi), \quad \forall \phi \in V^h,$$

where

$$a^h(U, \phi) = (\nabla U, \nabla \phi)_{\Omega_1 \cup \Omega_2} - (\langle \nabla_{\boldsymbol{n}} U \rangle, [\phi])_\Gamma - ([U], \langle \nabla_{\boldsymbol{n}} \phi \rangle)_\Gamma + (\lambda h^{-1}[U], [\phi])_\Gamma,$$

$$l(\phi) = (f, \phi)_\Omega,$$

with

$$\langle \nabla_{\boldsymbol{n}} v \rangle = \nabla_{\boldsymbol{n}} v_1 \qquad \text{on } \Gamma,$$

and where h is the local meshsize (3.1). The continuity conditions of u and $\nabla_{\boldsymbol{n}} u$ at Γ are satisfied weakly by means of a variant of Nitsche's method [10] for consistent weak enforcement of Dirichlet boundary conditions. To ensure stability, the parameter λ has to be taken sufficiently large and we return to this issue in Lemma 4.4 below.

Here we use a one sided approximation of the normal flux on the interface instead of the usual symmetric average

$$\langle \nabla_{\boldsymbol{n}} v \rangle = (\nabla_{\boldsymbol{n}} v_1 + \nabla_{\boldsymbol{n}} v_2)/2 \qquad \text{on } \Gamma,$$

commonly used in the discontinuous Galerkin method and in the context of interfaces between meshes that are shape regular on both sides of the interface by Becker, Hansbo & Stenberg [1]. The latter situation rules out the possibility of arbitrary small elements in Ω_2 close to the interface. As has been noted by Stenberg [12], any convex combination of the fluxes yields consistent methods. In Hansbo & Hansbo [7], this fact was exploited to allow for internal discontinuities along an interface in shape regular elements, chosing convex combinations that take into account the size of the parts of the cut element to ensure stability. In fact, a one-sided flux approximation could have been used there too, however with negligible gain in implementation complexity. Likewise, in the case of the present work a stable two-sided variant may be defined. However, in this case such a method but becomes more complicated to construct and implement since the element parts on each side of the interface now stems from two different meshes. This is an important practical point, and the main reason why we use one-sided fluxes here.

   With these definitions, we have the following consistency relation.

Proposition 3.1. *The discrete problem* (3.2) *is consistent in the sense that, for u solving* (2.1)–(2.2) *there holds*

$$a^h(u, \phi) = l(\phi), \quad \forall \phi \in V^h,$$

or, equivalently,

$$(3.3) \qquad\qquad a^h(u - U, \phi) = 0, \quad \forall \phi \in V^h.$$

Proof. Let u be the solution of the Poisson problem (2.1)–(2.2). Then $\langle \nabla_{\boldsymbol{n}} u \rangle = n_1 \nabla \cdot u_1 = -n_2 \nabla \cdot u_2 = \nabla_{\boldsymbol{n}} u$ and $[u] = 0$. By Green's formula it follows that

$$
\begin{aligned}
a^h(u, \phi) &= (\nabla u, \nabla \phi)_{\Omega_1 \cup \Omega_2} - (\langle \nabla_{\boldsymbol{n}} u \rangle, [\phi])_\Gamma \\
&= (-\Delta u, \phi)_{\Omega_1 \cup \Omega_2} + (\nabla_{\boldsymbol{n}} u - \langle \nabla_{\boldsymbol{n}} u \rangle, [\phi])_\Gamma = (f, \phi)_{\Omega_1 \cup \Omega_2},
\end{aligned}
$$

which proves the result. $\square$

4. A Priori Analysis

4.1. **Interpolation Error Estimates.** In the error analysis, we shall use the following mesh dependent norms:

$$\|v\|_{1/2,h,\Gamma}^2 := \|h(x)^{-1/2} v\|_{0,\Gamma}^2 = \sum_{j \in J_h} h_{K_1^j}^{-1} \|v\|_{0,\Gamma^j}^2,$$

$$\|v\|_{-1/2,h,\Gamma}^2 := \|h(x)^{1/2} v\|_{0,\Gamma}^2 = \sum_{j \in J_h} h_{K_1^j} \|v\|_{0,\Gamma^j}^2,$$

and

$$(4.1) \qquad \||v\||^2 := \|\nabla v\|_{0,\Omega_1 \cup \Omega_2}^2 + \|\langle \nabla_{\boldsymbol{n}} v \rangle\|_{-1/2,h,\Gamma}^2 + \|[v]\|_{1/2,h,\Gamma}^2.$$

Note for future reference that

$$(4.2) \qquad\qquad (u, v)_\Gamma \leq \|v\|_{1/2,h,\Gamma} \|v\|_{-1/2,h,\Gamma}.$$

   To show that functions in V^h approximates functions $v \in H_0^1(\Omega) \cap H^{p+1}(\Omega)$ to the order h^p in the norm $\|| \cdot \||$, we define an interpolant $I^h v \in V^h$ of v by $I^h v = I_i^h v$ on Ω_i, $i = 1, 2$.

Here I_i^h is the standard Lagrange nodal interpolant on the mesh T_i^h of Ω_i^*. The following local interpolation error estimates holds, see, e.g., [3].

$$(4.3) \qquad \|v - I_i^h v\|_{m,K} \le C h_K^{p+1-m} |v|_{p+1,K}, \quad m = 0, 1, \ p \ge 1, \ K \in T_h^i, i = 1, 2.$$

One may note that a node of interpolation used to define $I_2^h v$ lies in $\overline{\Omega_2^*} = \cup_{K \in T_2^h} \overline{K}$ but not necessarily in $\overline{\Omega_2}$.

The following interpolation error estimate holds.

Lemma 4.1. *Let $I^h v = I_i^h v$ on Ω_i, $i = 1, 2$, where I_i^h is the Lagrange nodal interpolant on the mesh T_i^h of Ω_i^*. Then, for $p \ge 1$,*

$$(4.4) \qquad \||v - I^h v\|| \le C h^p |v|_{p+1,\Omega}, \quad \forall v \in H_0^1(\Omega) \cap H^{p+1}(\Omega).$$

In the proof of this result, we need to estimate the interpolation error at the interface. We recall the well known trace inequality

$$(4.5) \qquad \|w\|_{0,\partial \tilde{K}}^2 \le C \|w\|_{0,\tilde{K}} \|w\|_{1,\tilde{K}}, \quad \forall w \in H^1(\tilde{K}).$$

on a reference element $\tilde{K}$. The following Lemma provides a scaled version of (4.5) which can be used to estimate traces not only on the boundary but on arbitrary lines (planes) intersecting the element.

Lemma 4.2. *Let L be the intersection between a line (plane) and an element K. Then*

$$(4.6) \qquad \|w\|_{0,L}^2 \le C h_K^{-1} \|w\|_{0,K}^2 + h_K \|w\|_{1,K}^2, \quad \forall w \in H^1(K),$$

where the constant C is independent of L.

Proof. Map the element by an affine map to a reference element $\tilde{K}$ and denote by $\tilde{L}$ the image of L. For the plane case, let (ξ, η) denote local coordinates on $\tilde{K}$ such that $\eta = 0$ on $\tilde{L}$. If $\tilde{L}$ divides $\tilde{K}$ into two subsets let $\tilde{K}_1$ denote one of these sets, and else set $\tilde{K}_1 = \tilde{K}$. Let $\boldsymbol{n}$ denote the outward pointing unit normal of $\tilde{K}_1$ and note that we may assume that $n_\eta = 1$ on $\tilde{\Gamma}$. By the divergence theorem,

$$\begin{aligned} 2 \int_{\tilde{K}_1} w \frac{\partial w}{\partial \zeta} \, dV &= \int_{\tilde{K}_1} \mathrm{div}\,(0, w^2) \, dV = \int_{\partial \tilde{K}_1} \boldsymbol{n} \cdot (0, w^2) \, dA \\ &= \int_{\tilde{L}} w^2 \, dA + \int_{\partial \tilde{K}_1 \setminus \tilde{L}} n_\eta w^2 \, dA. \end{aligned}$$

We thus find, using Cauchy-Schwarz' inequality and (4.5), that

$$\begin{aligned} \|w\|_{0,\tilde{L}}^2 &\le 2 \|w\|_{0,\tilde{K}_1} \|w\|_{1,\tilde{K}_1} + \|w\|_{0,\partial \tilde{K}_1 \setminus \tilde{L}}^2 \\ &\le 2 \|w\|_{0,\tilde{K}_1} \|w\|_{1,\tilde{K}_1} + \|w\|_{0,\partial \tilde{K}}^2 \le C \|w\|_{0,\tilde{K}} \|w\|_{1,\tilde{K}}. \end{aligned}$$

The result of the lemma now follows by scaling. The proof in three dimensions is similar. $\square$

Proof of Lemma 4.1. Starting from the definition of the norm (4.1) we have three terms to estimate. Beginning with the interior contributions we find that

$$(4.7) \qquad \|\nabla(v - I^h v)\|_{0,\Omega_i} \leq \|\nabla(v - I_i^h v)\|_{0,\Omega_i^*} \leq Ch^p |v|_{p+1,\Omega_i^*} \leq Ch^p |v|_{p+1,\Omega},$$

for $i = 1, 2$. Here we have used the fact that $\Omega_i \subset \Omega_i^* \subset \Omega$ and the interpolation error estimate (4.3).

Next, for the contribution from the jump at the interface, we note that

$$(4.8) \qquad \|[v - I^h v]\|_{1/2,h,\Gamma} \leq \|v - I_1^h v\|_{1/2,h,\Gamma} + \|v - I_2^h v\|_{1/2,h,\Gamma}.$$

and consider first the second term on the right. Let $L(\Gamma_j)$ be the line segment (plane domain) obtained by extending Γ_j to the boundary of $K_2^j \in T_2^h$.

By the definition of the discrete 1/2-norm,

$$(4.9) \qquad \|v - I_2^h v\|_{1/2,h,\Gamma} \leq \sum_{K \in T_h^2} \sum_{\Gamma_j \subset K} h_{K_1^j}^{-1/2} \|v - I_2^h v\|_{0,L(\Gamma_j)}.$$

By Lemma 4.2, we have that

$$(4.10) \qquad h_{K_1^j}^{-1} \|v - I_2^h v\|_{0,L(\Gamma_j)}^2 \leq C h_{K_2^j} h_{K_1^j}^{-1} \left(h_{K_2^j}^{-2} \|v - I_2^h v\|_{0,K_2^j}^2 + \|v - I_2^h v\|_{1,K_2^j}^2 \right).$$

It follows from assumption A2 that $h_{K_2^j} h_{K_1^j}^{-1} \leq C$. Hence by (4.10) and the interpolation estimate (4.4) we obtain

$$(4.11) \qquad h_{K_1^j}^{-1} \|v - I_2^h v\|_{0,L(\Gamma^j)}^2 \leq Ch^{2p} |v|_{p+1,K_2^j}^2.$$

Combining (4.9) and (4.11) we arrive at the desired estimate

$$(4.12) \qquad \|v - I_2^h v\|_{1/2,h,\Gamma} \leq Ch^p |v|_{p+1,\Omega_2^*} \leq Ch^p |v|_{p+1,\Omega}.$$

Here we have used that by assumption A2, the number of terms in the inner sum in (4.9) is bounded, uniformly with respect to the mesh size. The estimate for the first term on the right hand side in (4.8) is readily found by similar arguments.

Finally, by Lemma 4.2 with $w = \langle \nabla_{\boldsymbol{n}} (v - I^h v) \rangle = \nabla_{\boldsymbol{n}} (v - I_1^h v)$, we have that

$$h_{K_1^j} \|\langle \nabla_{\boldsymbol{n}} (v - I^h v) \rangle\|_{0,L(\Gamma^j)}^2 \leq C \left(\|\nabla(v - I_1^h v)\|_{1,K_1^j}^2 + h_{K_1^j}^2 \|\nabla(v - I_1^h v)\|_{2,K_1^j}^2 \right).$$

We find in the same way as above, using the interpolation error estimate (4.4) and summing the contributions over the interface, that

$$(4.13) \qquad \|\langle \nabla_{\boldsymbol{n}} (v - I^h v) \rangle\|_{-1/2,h,\Gamma} \leq Ch^p |v|_{p+1,\Omega}.$$

The lemma now follows from (4.7), (4.12) and (4.13). $\qquad\qquad\qquad\qquad\qquad\qquad\square$

4.2. **Coercivity.** To prove coercivity of the bilinear form we need the following known inverse inequality. We include its proof for completeness.

Lemma 4.3. *For $\phi \in V^h$, the following inverse inequality holds:*

$$\|\langle \nabla_{\boldsymbol{n}} \phi \rangle\|^2_{-1/2,h,\Gamma} \leq C_I \|\nabla \phi\|^2_{0,\Omega_1}.$$

Proof. Recall the definition of $\langle \nabla_{\boldsymbol{n}} \phi \rangle = \nabla_{\boldsymbol{n}} \phi_1$. Note that on a reference triangle (tetrahedron) $\tilde{K}$ which is the image of $K \in T_1^h$ under an affine map, we have

$$\|\langle \nabla_{\boldsymbol{n}} \phi \rangle\|^2_{\tilde{\Gamma}} \leq C \|\nabla \phi\|^2_{0,\tilde{K}}.$$

since if the the right hand side is zero so is the left hand side, and since the space of polynomials of degree $p - 1$ is finite dimensional. The result then follows by scaling, using the invers of the affine map, and summation over all elements with an edge on the interface Γ. $\qquad\square$

Lemma 4.4. *The discrete form $a^h(\cdot, \cdot)$ is coercive on V^h, i.e.,*

$$a^h(v, v) \geq C \|\|v\|\|^2 \quad \forall v \in V^h,$$

provided λ is chosen sufficiently large. It is also continuous, i.e.,

$$a^h(u, v) \leq C \|\|u\|\| \, \|\|v\|\| \quad \forall u, v \in V.$$

Proof. Continuity of the discrete form follows directly from the definitions. To prove coercivity, we use (4.2) to estimate the form from above:

$$a^h(v, v) = \|\nabla v\|^2_{0,\Omega_1} + \|\nabla v\|^2_{0,\Omega_2} - 2([v], \langle \nabla_{\boldsymbol{n}} v \rangle)_\Gamma + \|\lambda^{1/2}[v]\|^2_{1/2,h,\Gamma}$$

$$\geq \|\nabla v\|^2_{0,\Omega_1} + \|\nabla v\|^2_{0,\Omega_2} - 2\|\langle \nabla_{\boldsymbol{n}} v \rangle\|_{-1/2,h,\Gamma}\|[v]\|_{1/2,h,\Gamma} + \lambda\|[v]\|^2_{1/2,h,\Gamma}.$$

It follows from the inverse inequality in Lemma 4.3 that

$$-2\|\langle \nabla_{\boldsymbol{n}} v \rangle\|_{-1/2,h,\Gamma}\|[v]\|_{1/2,h,\Gamma} \geq -\epsilon\|\{\nabla_{\boldsymbol{n}} v\}\|^2_{-1/2,h,\Gamma} - \epsilon^{-1}\|[v]\|^2_{1/2,h,\Gamma}$$

$$\geq -\epsilon C_I \|\nabla v\|^2_{0,\Omega_1} - \epsilon^{-1}\|[v]\|^2_{1/2,h,\Gamma}.$$

Combining these estimates we obtain

$$a^h(v, v) \geq (1 - \epsilon C_I)\|\nabla v\|^2_{0,\Omega_1} + \|\nabla v\|^2_{0,\Omega_2} + (\lambda - \epsilon^{-1})\|[v]\|^2_{1/2,h,\Gamma}.$$

Taking $\epsilon = 1/(2C_I)$, coercivity follows if $\lambda \geq 1/2 + 1/\epsilon$. $\qquad\square$

4.3. **A Priori Error Estimates.**

Theorem 4.1. *For U solving (3.2) and u solving (2.1–2.2), the following a priori error estimates hold*

$$(4.14) \qquad\qquad \|\|u - U\|\| \leq Ch^p |u|_{p+1,\Omega},$$

and

$$(4.15) \qquad\qquad \|u - U\|_{0,\Omega} \leq Ch^{p+1} |u|_{p+1,\Omega}.$$

ion10 ANITA HANSBO, PETER HANSBO, AND MATS G. LARSON

Proof. For any $v \in V^h$, $\||u - U\|| \leq \||u - v\|| + \||v - U\||$. Further, by Lemma 4.4 and orthogonality, we have that

$$
\begin{aligned}
\||U - v\||^2 &\leq C a^h(U - v, U - v) \\
&= C a^h(u - v, U - v) \\
&\leq C\||u - v\||\,\||U - v\||,
\end{aligned}
$$

and it follows that

$$
\||u - U\|| \leq C\||u - v\|| \quad \forall v \in V^h.
$$

Taking $v = I^h u$ and invoking the interpolation result of Theorem 4.1, (4.14) follows.

For (4.15) we use a duality argument. Let z be defined by

$$
(4.16) \qquad \begin{aligned} -\Delta z &= e \quad \text{in } \Omega, \\ z &= 0 \quad \text{on } \partial\Omega, \end{aligned}
$$

with $e = u - U$. Multiplying (4.16) with e and using Green's formula gives

$$
\begin{aligned}
\|e\|_{0,\Omega}^2 &= -(\Delta z, e)_\Omega \\
&= (\nabla z, \nabla e)_{\Omega_1} + (\nabla z, \nabla e)_{\Omega_2} - (\nabla_{\boldsymbol{n}} z, [e])_\Gamma \\
&= a^h(z, e),
\end{aligned}
$$

since $[z] = 0$ and $\nabla_{\boldsymbol{n}} z = \langle \nabla_{\boldsymbol{n}} z \rangle$. Now, using the symmetry of $a^h(\cdot, \cdot)$, the orthogonality relation (3.3), and Theorem 4.1, we find that

$$
(4.17) \qquad \|e\|_{0,\Omega}^2 = a^h(z - I^h z, e) \leq C\||z - I^h z\||\,\||e\|| \leq Ch\|z\|_{2,\Omega}\||e\||.
$$

Finally, by elliptic regularity, we have

$$
\|z\|_{2,\Omega} \leq C\|e\|_{0,\Omega},
$$

and thus the estimate (4.15) follows from (4.14) and (4.17). $\qquad\square$

5. A Posteriori Error Estimates

We first introduce an interpolation operator suitable for the a posteriori error analysis. From Scott and Zhang [11] we deduce the existence of Clement type interpolation operators $r_{h,i}$, $i = 1, 2$, defined on $H^1(\Omega_i^*)$, which preserve Dirichlet boundary conditions on $\partial\Omega \cap \overline{\Omega_i^*}$ and satisfy the following local interpolation error estimates.

$$
(5.1) \qquad h_K^{m-1}\|r_{h,i}v - v\|_{m,K} \leq C\|\nabla v\|_{0,\Delta K}, \quad m = 0, 1, \ K \in T_{h,i}.
$$

Here ΔK denotes a patch of elements which are neighbors of K. We then define

$$
(5.2) \qquad \pi v := (r_{h,1}v_1, (r_{h,2}\mathsf{E}_2 v_2)|_{\Omega_2}) \quad \text{for } v \in H^1(\Omega_1 \cup \Omega_2).
$$

Here we have used an extension operator $\mathsf{E}_2 : H^1(\Omega_2) \to H^1(\Omega)$ such that $(\mathsf{E}_2 w)|_{\Omega_2} = w$ and

$$
(5.3) \qquad |\mathsf{E}_2 w|_{m,\Omega} \leq C|w|_{m,\Omega_i} \quad \forall w \in H^m(\Omega_2), \quad m = 0, 1.
$$

In the following lemma we collect some useful estimates for the interpolation operator π.

Lemma 5.1. *Let π be the interpolation operator defined in (5.2). Under assumptions A1 and A2 the following estimates hold for $v \in H^1(\Omega_1 \cup \Omega_2)$:*

$$(5.4) \qquad \sum_{K \in T_i^h} h_K^{-2} \|v_i - (\pi v)_i\|_{K \cap \Omega_i}^2 \leq C\|\nabla v_i\|_{0,\Omega_i}^2, \quad i = 1, 2,$$

$$(5.5) \qquad \|v_i - (\pi v)_i\|_{1/2,h,\Gamma} \leq C\|\nabla v_i\|_{0,\Omega_i}, \quad i = 1, 2,$$

$$(5.6) \qquad \sum_{K \in T_i^h} h_K^{-1} \|v - \pi v\|_{0,\partial(K \cap \Omega_i) \backslash \Gamma}^2 \leq C\|\nabla v_i\|_{0,\Omega_i}^2, \quad i = 1, 2,$$

$$(5.7) \qquad \|\nabla(\pi v)\|_{0,\Omega_i} \leq C\|\nabla v\|_{0,\Omega_i}, \quad i = 1, 2.$$

Proof. We consider the case $i = 2$ as the proof for $i = 1$ is similar. Let $v_2^* = \mathsf{E}_2 v_2$ denote the extension of v_2 to Ω and recall that $v_2 - (\pi v)_2 = v_2^* - r_{h,2} v_2^*$ on Ω_2. Using (5.1) with $m = 0$ we obtain, for $K \in T_2^h$, that

$$h_K^{-1} \|v_2 - (\pi v)_2\|_{0,K \cap \Omega_2} \leq \|v_2^* - r_{h,2} v_2^*\|_{0,K} \leq C\|\nabla v_2^*\|_{0,\Delta K},$$

As the number of elements in the patches ΔK is uniformly bounded with respect to the mesh size by assumption A1, it follows that

$$\sum_{K \in T_i^h} h_K^{-2} \|v_i - (\pi v)_i\|_{K \cap \Omega_2}^2 \leq C\|\nabla v_2^*\|_{0,\Omega_2^*}^2,$$

whence (5.4) follows by the bound for the extentions operator (5.3). Turning to the second inequality (5.5) of the lemma, it follows from trace inequality (4.6) and interpolation estimate (5.4) that

$$\begin{aligned} h_{K_1^j}^{-1} \|v_2 - (\pi v)_2\|_{0,\Gamma^j}^2 &\leq C h_{K_2^j}^{-2} \|v_2 - (\pi v)_2\|_{0,K_2}^2 + \|v_2 - (\pi v)_2\|_{1,K_2}^2 \\ &\leq C\|\nabla v_2\|_{0,\Delta K_2}^2, \end{aligned}$$

where we also have used that $h_{K_2^j} h_{K_1^j}^{-1} \leq C$ by assumption A2. Summing over the elements and using (5.3) gives

$$\|v_2 - (\pi v)_2\|_{1/2,h,\Gamma} \leq C\|\nabla v_2^*\|_{0,\Omega_2^*} \leq C\|\nabla v\|_{0,\Omega_2}.$$

The third estimate (5.6) is readily shown by similar arguments. Finally, for the fourth inequality of the lemma, it follows from (5.1) and (5.3) that

$$\|\nabla(\pi v)\|_{0,\Omega_2} \leq \|\nabla(v_2^* - r_{h,2} v_2^*)\|_{0,\Omega_2^*} + \|\nabla v\|_{0,\Omega_2} \leq C\|\nabla v\|_{0,\Omega_2},$$

and the proof is complete. $\qquad\square$

We shall also need the following trace inequality.

Lemma 5.2. *Under our mesh assumptions there holds, for all $K \in T_1^h$ and $\Gamma_j \subset \partial K$,*

$$(5.8) \qquad \|\nabla_{\boldsymbol{n}} v_1\|_{-1/2,\Gamma^j} \leq C\Big(\|\nabla v_1\|_{0,K} + h_K\|\Delta v_1\|_{0,K}\Big), \quad v \in H^2(K).$$

Proof. On a reference element $\tilde{K}$ there holds (cf. [6], Theorem 2.2)

$$\|\boldsymbol{n} \cdot w\|_{-1/2, \partial \tilde{K}} \leq C\Big(\|w\|_{0,\tilde{K}} + \|\nabla \cdot w\|_{0,\tilde{K}}\Big), \quad w \in L_2(\tilde{K})^n : \nabla \cdot w \in L_2(\tilde{K}).$$

The result follows from this estimate, scaled by the map from the reference element, with $w = \nabla v$.   □

We are now ready to show an a posteriori error estimate in a discrete energy norm, using the following notation. At an edge of an element K that is common with a neighbouring element L we let $[w] = w|_K - w|_L$ denote the jump of w over the edge. Further, $\boldsymbol{n}_P$ denotes the outward pointing unit normal of the boundary of a domain P.

Theorem 5.1. *Assume A1, A2, and $\lambda \geq 1$. For U solving (3.2) and u solving (2.3), the following a posteriori error estimate holds :*

$$(5.9) \qquad \|\nabla e\|_{0,\Omega_1 \cup \Omega_2}^2 + \|[e]\|_{1/2,h,\Gamma}^2 \leq C \sum_{i=1}^{2} \sum_{K \in T_i^h} \rho_{K,i}^2.$$

Here the element error indicators $\rho_{K,i}$ are defined by

$$\rho_{K,i}^2 = h_K^2 \|f + \Delta U\|_{0,P_K}^2 + h_K \|[\boldsymbol{n}_{P_K} \cdot \nabla U]\|_{0,\partial P_K}^2 + h_K^{-1} \|[U]\|_{0,\partial P_K \cap \Gamma}^2 + \sum_{\Gamma_j \subset \overline{K}} \|[U]\|_{1/2,\Gamma_j}^2,$$

where $P_K = K \cap \Omega_i$ for $K \in T_i^h$.

Proof. Using the definition of the method (3.2) we have the identity
(5.10)
$$I = (\nabla e, \nabla e)_{\Omega_1 \cup \Omega_2} = (\nabla e, \nabla(e - \pi e))_{\Omega_1 \cup \Omega_2} + (\langle \nabla_{\boldsymbol{n}} e \rangle, [\pi e])_\Gamma + ([e], \langle \nabla_{\boldsymbol{n}} \pi e \rangle)_\Gamma - (\lambda h^{-1}[e], [\pi e])_\Gamma.$$

Integration by parts gives

$$
\begin{aligned}
(5.11) \qquad I \ = \ & \sum_{i=1}^{2} \sum_{K \in T_i^h} \left((-\Delta e, (e - \pi e))_{P_K} + \frac{1}{2}([\boldsymbol{n}_K \cdot \nabla e], e - \pi e)_{\partial P_K \backslash \Gamma} \right) \\
& + (\langle \nabla_{\boldsymbol{n}} e \rangle, [e - \pi e])_\Gamma + ([\nabla_{\boldsymbol{n}} e], e_2 - \pi e_2)_\Gamma \\
& + (\langle \nabla_{\boldsymbol{n}} e \rangle, [\pi e])_\Gamma + ([e], \langle \nabla_{\boldsymbol{n}} \pi e \rangle)_\Gamma - (\lambda h^{-1}[e], [\pi e])_\Gamma.
\end{aligned}
$$

Note that we may write

$$-(\lambda h^{-1}[e], [\pi e])_\Gamma = (\lambda h^{-1}[e], [e - \pi e])_\Gamma - \|[e]\|_{1/2,h,\Gamma}^2 - ((\lambda - 1)h^{-1}[e], [e])_\Gamma.$$

Using that u and its derivatives have zero jumps over the element edges and the interface, and also that $-\Delta e = f + \Delta U$ in the interior of the elements, we obtain the error

representation formula

$$\|\nabla e\|_{0,\Omega_1\cup\Omega_2}^2 + \|[e]\|_{1/2,h,\Gamma}^2 \;=\; \sum_{i=1}^{2}\sum_{K\in T_i^h}\left((f+\Delta U,(e-\pi e))_{P_K} + \frac{1}{2}([\mathbf{n}_K\cdot\nabla U],e-\pi e)_{\partial P_K\backslash\Gamma}\right)$$
$$+([\nabla_{\mathbf{n}}U],e_2-\pi e_2)_\Gamma + ([U],\langle\nabla_{\mathbf{n}}e\rangle)_\Gamma + ([U],\langle\nabla_{\mathbf{n}}\pi e\rangle)_\Gamma$$
$$+(\lambda h^{-1}[U],[e-\pi e])_\Gamma - ((\lambda-1)h^{-1}[e],[e])_\Gamma.$$

Here the last term is non-positive under our assumptions. We now proceed to estimate the other terms on the right hand side. For $\epsilon > 0$ to be chosen below we have that

$$(f+\Delta U,(e-\pi e))_{P_K} \le \|(f+\Delta U\|_{0,P_K}\|e-\pi e\|_{0,P_K}$$
$$\le \frac{1}{2\epsilon}h_K^2\|f+\Delta U\|_{0,P_K}^2 + \frac{\epsilon}{2}h_K^{-2}\|e-\pi e\|_{0,P_K}^2.$$

Treating the other term in the sum over the elements in the same way, we find by Lemma 5.1 that the first term in (5.12) may be estimated as follows.

$$\sum_{K\in T_i^h}\left((f+\Delta U,(e-\pi e))_{P_K} + \frac{1}{2}([\mathbf{n}_K\cdot\nabla U],e-\pi e)_{\partial P_K\backslash\Gamma}\right)$$
$$\le \frac{C}{\epsilon}\sum_{K\in T_i^h}\left(h_K^2\|f+\Delta U\|_{0,P_K}^2 + h_K\|[\mathbf{n}_K\cdot\nabla U]\|_{0,\partial P_K\backslash\Gamma}^2\right)$$
$$+C\epsilon\sum_{K\in T_i^h}\left(h_K^{-2}\|e-\pi e\|_{0,P_K}^2 + h_K^{-1}\|e-\pi e\|_{0,\partial P_K\backslash\Gamma}^2\right)$$
$$\le \frac{C}{\epsilon}\sum_{K\in T_i^h}\left(h_K^2\|f+\Delta U\|_{0,P_K}^2 + h_K\|[\mathbf{n}_K\cdot\nabla U]\|_{0,\partial P_K\backslash\Gamma}^2\right)$$
$$(5.12) \qquad\qquad +C\epsilon\|\nabla e\|_{0,\Omega_i}^2.$$

Using again Lemma 5.1, we obtain for the second term $([\nabla_{\mathbf{n}}U],e_2-\pi e_2)_\Gamma$ that

$$([\nabla_{\mathbf{n}}U],e_2-\pi e_2)_\Gamma \le C\|[\nabla_{\mathbf{n}}U]\|_{-1/2,h,\Gamma}\|e_2-\pi e_2\|_{1/2,h,\Gamma}$$
$$\le C\|[\nabla_{\mathbf{n}}U]\|_{-1/2,h,\Gamma}\|\nabla e\|_{0,\Omega_2}$$
$$\le \frac{C}{\epsilon}\|[\nabla_{\mathbf{n}}U]\|_{-1/2,h,\Gamma}^2 + C\epsilon\|\nabla e\|_{0,\Omega_2}^2$$
$$(5.13) \qquad\qquad \le \frac{C}{2\epsilon}\sum_{i=1}^{2}\sum_{K\in T_i^h}h_K\|[\nabla_{\mathbf{n}}U]\|_{\partial P_K\cap\Gamma}^2 + C\epsilon\|\nabla e\|_{0,\Omega_2}^2.$$

In the last step above, we have merely distributed the error indicator at Γ over the elements intersected by Γ, using that the element sizes are compatible by assumption A2. For the

third term $([U], \langle \nabla_{\boldsymbol{n}} e \rangle)_\Gamma$, we begin to note that

$$([U], \langle \nabla_{\boldsymbol{n}} e \rangle)_\Gamma \leq \sum_j \|[U]\|_{1/2,\Gamma_j} \|\nabla_{\boldsymbol{n}} e_1\|_{-1/2,\Gamma_j}$$

$$\leq \sum_j \frac{1}{2\epsilon} \|[U]\|^2_{1/2,\Gamma_j} + \frac{\epsilon}{2} \|\nabla_{\boldsymbol{n}} e_1\|^2_{-1/2,\Gamma_j}.$$

By the trace inequality of Lemma 5.2 we have that

$$\|\nabla_{\boldsymbol{n}} e_1\|^2_{-1/2,\Gamma_j} \leq C(\|\nabla e\|^2_{0,K_1^j} + h^2_{K_1^j} \|\nabla \cdot \nabla e\|^2_{0,K_1^j})$$

$$= C(\|\nabla e\|^2_{0,K_1^j} + h^2_{K_1^j} \|f + \Delta U\|^2_{0,K_1^j}),$$

and hence, since the number of parts Γ_j in each element is uniformly bounded,
(5.14)

$$
\begin{aligned}
([U], \langle \nabla_{\boldsymbol{n}} e \rangle)_\Gamma &\leq \frac{C}{\epsilon} \sum_j \left(h^2_{K_1^j} \|f + \Delta U\|^2_{0,K_1^j} + \|[U]\|^2_{1/2,\Gamma_j} \right) + C\epsilon \|\nabla e\|^2_{0,\Omega_1} \\
&\leq \frac{C}{\epsilon} \sum_{i=1}^2 \sum_{K \in T_i^h} \left(h^2_K \|f + \Delta U\|^2_{0,K_1^j} + \sum_{\Gamma_j \subset \overline{K}} \|[U]\|^2_{1/2,\Gamma_j} \right) + C\epsilon \|\nabla e\|^2_{0,\Omega_1}.
\end{aligned}
$$

The fourth term $([U], \langle \nabla_{\boldsymbol{n}} \pi e \rangle)_\Gamma$ is bounded as follows

$$([U], \langle \nabla_{\boldsymbol{n}} \pi e \rangle)_\Gamma \leq \|[U]\|_{1/2,h,\Gamma} \|\langle \nabla_{\boldsymbol{n}} \pi e \rangle\|_{-1/2,h,\Gamma}.$$

Further using the inverse inequality of Lemma 4.3 and (5.7) we obtain

$$\|\langle \nabla_{\boldsymbol{n}} \pi e \rangle\|_{-1/2,h,\Gamma} \leq C \|\nabla \pi e\|^2_{0,\Omega_1} \leq C \|\nabla e\|^2_{0,\Omega_1}.$$

Likewise, for the fifth and last term we find by Lemma 5.1 that

$$(h^{-1}[U], [e - \pi e])_\Gamma \leq \|[U]\|_{1/2,h,\Gamma} \|[e - \pi e]\|_{1/2,h,\Gamma} \leq C \|[U]\|_{1/2,h,\Gamma} \|\nabla e\|_{0,\Omega_1 \cup \Omega_2}.$$

Thus we get for the fourth and fifth terms that
(5.15)

$$
\begin{aligned}
([U], \langle \nabla_{\boldsymbol{n}} \pi e \rangle)_\Gamma + (h^{-1}[U], [e - \pi e])_\Gamma &\leq C \|[U]\|_{1/2,h,\Gamma} \|\nabla e\|_{0,\Omega_1 \cup \Omega_2} \\
&\leq \frac{C}{\epsilon} \sum_{i=1}^2 \sum_{K \in T_i^h} h^{-1}_K \|[U]\|^2_{0,\partial P_K \cap \Gamma} + C\epsilon \|\nabla e\|^2_{0,\Omega_1 \cup \Omega_2}.
\end{aligned}
$$

Choosing ϵ small enough, the theorem now follows from (5.12), (5.12), (5.13), (5.14), and (5.15). $\qquad \square$

The error indicator of Theorem 5.1 contains a term $D_K := h_K^{-1} \|[U]\|^2_{0,\partial P_K \cap \Gamma}$ corresponding to a discrete 1/2-norm over Γ, as well as a term

$$S_K := \sum_{\Gamma_j \subset \overline{K}} \|[U]\|^2_{1/2,\Gamma_j}$$

with continuous 1/2-norms over the parts Γ_j. We shall consider the computation of S_K in the special case of linear elements in two dimensions in Section 5 below, using that for a one-dimensional interface (see, e.g., [3])

$$(5.16) \qquad \|[U]\|^2_{1/2,\Gamma_j} := \|[U]\|^2_{0,\Gamma_j} + \int_{\Gamma_j} \int_{\Gamma_j} \frac{|[U](\xi) - [U](\eta)|^2}{|\xi - \eta|^2} d\xi \, d\eta.$$

In a general case, however, S_K is somewhat complicated to compute and one would like to simplify the error indicators. Indeed, S_K is bounded by (but not equal to) $\|[U]\|^2_{1/2,\partial P_K \cap \Gamma}$, and it is therefore natural to ask if an inverse inequality can be found which would make possible to remove S_K from the error indicator. We note that even though we have the inverse inequality $\|[U]\|^2_{1/2,\Gamma_j} \leq C|\Gamma_j|^{-1}\|[U]\|^2_{0,\Gamma_j}$, the corresponding elementwise inverse inequality $\|[U]\|^2_{1/2,\partial P_K \cap \Gamma} \leq Ch_K^{-1}\|[U]\|^2_{0,\partial P_K \cap \Gamma}$ does not follow since the parts Γ_j may become arbitrarily small even when the meshsize is bounded away from zero. Nevertheless, S_K and D_K may, as we shall show, both be bounded by a third quantity of the same order of magnitude. In Theorem 5.2 below we use this and some further simplifications to obtain a less sharp but more implementation-friendly a posterori error estimate. Integration over the parts P_K is not required to compute these error indicators, nor is integration over the parts Γ_j; all terms are integrals of single polynomials over the original elements or its edges.

Theorem 5.2. *For any piecewise polynomial w on the partition $\{\Gamma_j\}$ of Γ, let w_j denote the polynomal which defines w on Γ_j. Theorem 5.1 holds with $\rho^2_{K,i}$ replaced by*

$$\begin{aligned}\theta^2_{K,i} &= h^2_K \|f + \Delta U\|^2_{0,K} + h_K \|[\boldsymbol{n}_K \cdot \nabla U]\|^2_{0,\partial K \cap \Omega^*_i} \\ &\quad + \sum_{j:\Gamma_j \subset \overline{K}} \left(h_K \|[\nabla_{\boldsymbol{n}} U]_j\|^2_{0,\partial K_1^j \cap \Gamma} + h_K^{-1} \|[U]_j\|^2_{0,\partial K_1^j \cap \Gamma} \right).\end{aligned}$$

Proof. We shall show that $\rho_{K,i} \leq C\theta_{K,i}$. Obviously,

$$(5.17) \qquad \|f + \Delta U\|^2_{0,P_K} \leq \|f + \Delta U\|^2_{0,K}.$$

Further, for $K \in T_i^h$ we have that

$$h_K \|[\boldsymbol{n}_{P_K} \cdot \nabla U]\|^2_{0,\partial P_K} = h_K \|[\boldsymbol{n}_K \cdot \nabla U]\|^2_{0,\partial P_K \backslash \Gamma} + \sum_{\Gamma_j \subset \overline{K}} h_K \|[\boldsymbol{n}_{P_K} \cdot \nabla U]\|^2_{0,\Gamma_j}$$

$$(5.18) \qquad \leq h_K \|[\boldsymbol{n}_K \cdot \nabla U]\|^2_{0,\partial K \cap \Omega^*_i} + h_K \sum_{j:\Gamma_j \subset \overline{K}} \|[\boldsymbol{n} \cdot \nabla U]_j\|^2_{0,\partial K_1^j \cap \Gamma}.$$

We now turn to the estimate of $S_K = \sum_{\Gamma_j \subset \overline{K}} \|[U]\|^2_{1/2,\Gamma_j}$. For $K \in T_i^h$ and $\Gamma_j \subset \overline{K}$ we also have $\Gamma_j \subset \overline{K}_1^j$. Consider a reference element $\tilde{K}$ for K_1^j with Γ_j mapped onto $\tilde{\Gamma}_j$ in the edge (side) $\tilde{E}$. By equivalence of norms there holds for all polynomials q of degree p

$$\|q\|^2_{1/2,\tilde{\Gamma}_j} \leq \|q\|^2_{1/2,\tilde{E}} \leq C\|q\|^2_{0,\tilde{E}}.$$

Mapping back to K_1^j and taking $q = [U]_j$ we find that

$$\|[U]_j\|_{1/2,\Gamma_j}^2 \leq Ch_{K_1^j}^{-1}\|[U]_j\|_{0,\partial K_1^j \cap \Gamma}^2,$$

where the constant is independent of j. Hence, using assumption A2 to replace $h_{K_1^j}$ by h_K if $i = 2$,

$$(5.19) \qquad S_K \;=\; \sum_{\Gamma_j \subset \overline{K}} \|[U]\|_{1/2,\Gamma_j}^2 \leq Ch_K^{-1} \sum_{j:\Gamma_j \subset \overline{K}} \|[U]_j\|_{0,\partial K_1^j \cap \Gamma}^2.$$

Since $D_K = h_K^{-1}\|[U]\|_{0,\partial P_K \cap \Gamma}^2$ is indeed bounded by the right hand side above, the theorem now follows from (5.17), (5.18), and (5.19). $\qquad\qquad\qquad\qquad\qquad\qquad\square$

6. Numerical examples

6.1. **Implementation.** For the numerical examples to be presented, we chose to make the following simplifying assumption: the interface is assumed to be made up of straight lines that are so long that each element on the cut grid is intersected by just one corner of the interface. We further assumed that the area enclosed by the interface lay completely within the cut mesh. We then needed to consider only seven cases, depicted in Figures 3-5.
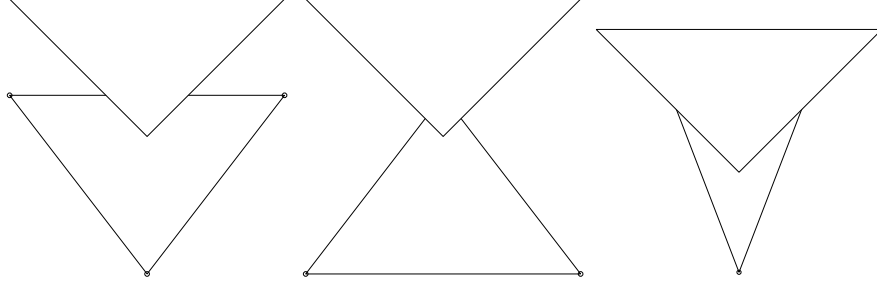

FIGURE 3. Elements containing one corner of the interface: zero nodes, one node, and two nodes on the opposite side of the interface.
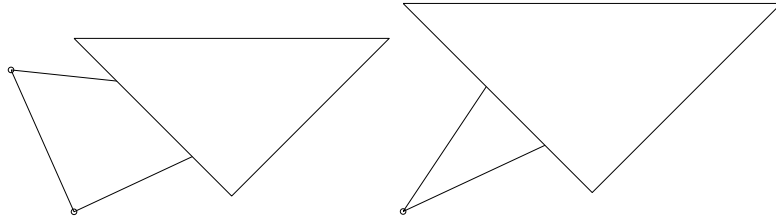

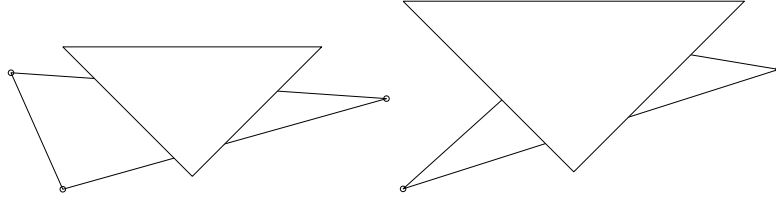FIGURE 4. Elements cut by a straight segment: one node and two nodes on the opposite side of the interface.

FIGURE 5. Overlapped elements: two sides and three sides cut.

For the numerical integration, we divided any non-triangular cut part of an element into triangles, using sufficiently high integration for the stiffness matrix to be exactly evaluated. On the interface we performed exact (numerical) integration of all terms using the union of the intersection points on the cut side and the nodes on the uncut side to define the intervals of integration.

6.2. **Convergence study.** The example was solved on the domain $(-4, 4) \times (-4, 4)$ with an overlapping domain according to Figure 6. The locations of the corners of the overlapping domain were determined by

$$\begin{bmatrix} x \\ y \end{bmatrix} = \begin{bmatrix} \cos\phi & -\sin\phi \\ \sin\phi & \cos\phi \end{bmatrix} \begin{bmatrix} -2.5 & 0.5 & 0.5 & -2.5 \\ -2.5 & -2.5 & 0.5 & 0.5 \end{bmatrix} + \begin{bmatrix} 0.75 \\ 1 \end{bmatrix},$$

with $\phi = 1$.

We imposed zero Dirichlet boundary conditions and applied a forcing term

$$f = 64 - 2\,x^2 - 2\,y^2,$$

corresponding to the exact solution

$$u = (x - 4)\,(x + 4)\,(y - 4)\,(y + 4).$$

We solved this problem numerically using finite elements with both a linear and a quadratic polynomial *ansatz*. Elevations of the different solutions on the same mesh can be seen in Figure 7. In Figure 8, we show the convergence in L_2–norm of on a sequence of refined meshes. As expected, we obtain second and third order convergence for the linear and quadratic approximations, respectively.

6.3. **Adaptive refinement.** In order to evaluate the a posteriori estimate (5.9) we need to compute the continuous half-norm (5.16) of the jump. We have implemented the error estimator for linear elements, whence we compute the half-norm as follows: since $[U]$ is linear on each Γ_j, $[U](\xi) = a\xi + b$, say, we can write

$$\frac{|[U](\xi) - [U](\eta)|^2}{|\xi - \eta|^2} = \frac{|a\,(\xi - \eta)|^2}{|\xi - \eta|^2} = a^2$$

and thus

$$\|[U]\|_{1/2,\Gamma_j}^2 = \|[U]\|_{0,\Gamma_j}^2 + a^2|\Gamma_j|^2.$$
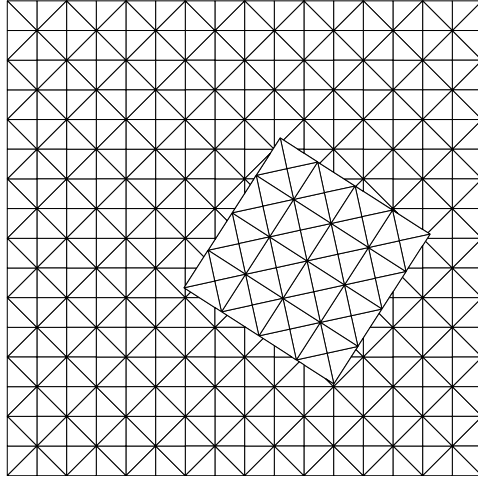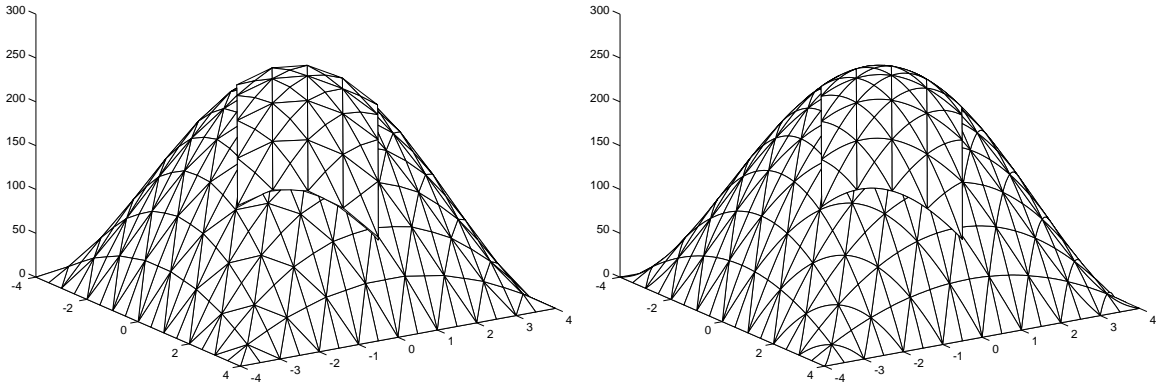
FIGURE 6. Coarse triangulation of the domains.

FIGURE 7. Elevation of the linear and the quadratic solutions on the coarse mesh.

We considered an example with exact solution

$$u = \frac{1}{256} e^{-(x^2+y^2)} (4 - x)(4 + x)(4 - y)(4 + y),$$

on the same domain as in the previous example, and used the two a posteriori estimates of Theorem 5.1, called estimate 1, and Theorem 5.2, called estimate 2. These estimates were used to control the local meshsize by a fixed fraction refinement strategy (refining the elements containing the largest contributions). No attempt was made to calibrate the unknown constants appearing
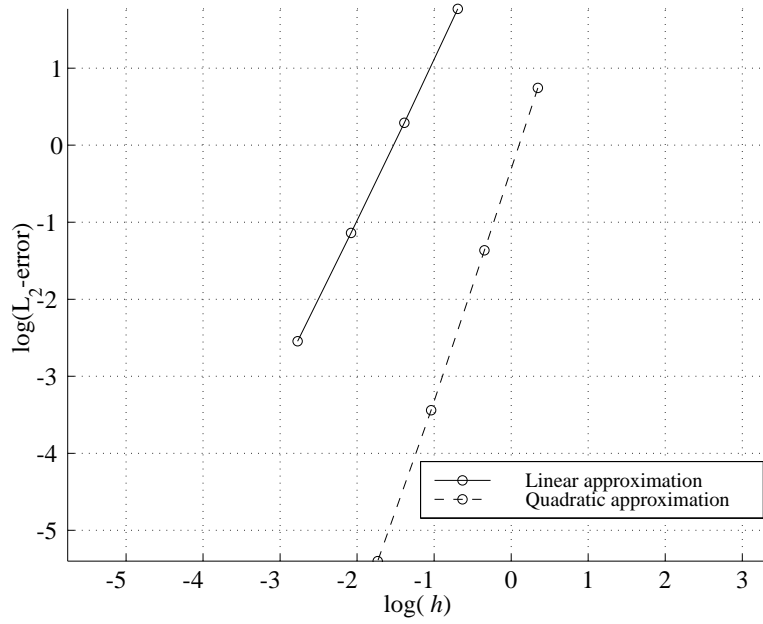
FIGURE 8. Convergence of the different approximations.

in the estimates; instead we computed the effectivity index, defined as

$$\text{effectivity index} = \frac{\text{estimated error}}{\text{exact error}},$$

in order to numerically verify that it remained constant as the mesh was refined. In Figure 9, we show the mesh obtained when using estimate 1, and in Figure 10 the corresponding result when using estimate 2. The solution on this mesh is shown as an elevation in Figure 11. Note that the meshes in both cases has a tendency to refine more at the interface. This is because the local error is the largest there, as has been noted previously, cf. [1, 7]. This phenomenon is more noticeable using estimate 2, as expected since this estimate is more conservative at the interface. Finally, in Figure 12, we show the effectivity index on the sequence of meshes for both estimators. As can be seen, the effectivity index is almost constant for both estimates, which indicates that the refinement on the interface does not much affect the global norm. We also show the ratio of the errors on the sequence of meshes obtained with estimate 2 to that obtained with estimate 1. We note that this ratio is slightly above 1, indicating that the degrees of freedom are put to slightly better use using estimate 1, as expected.
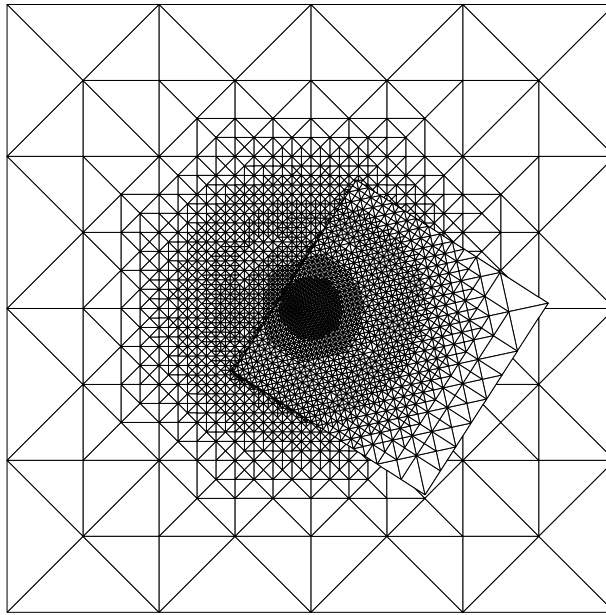
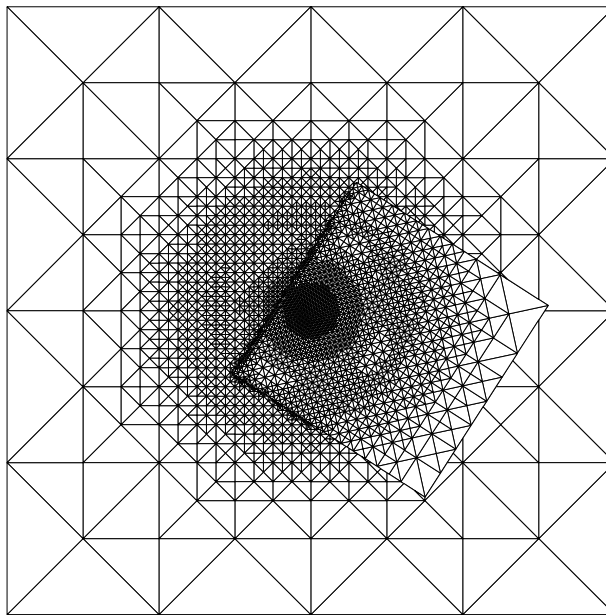FIGURE 9. Final adapted mesh in a sequence using Estimate 1.

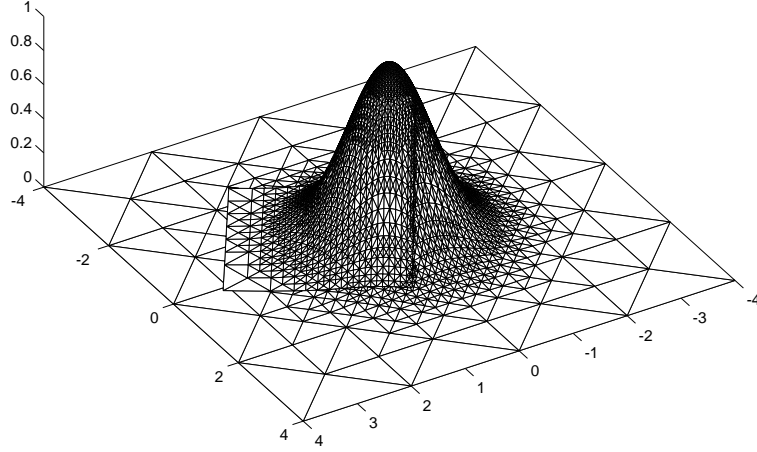FIGURE 10. Final adapted mesh in a sequence using Estimate 2.
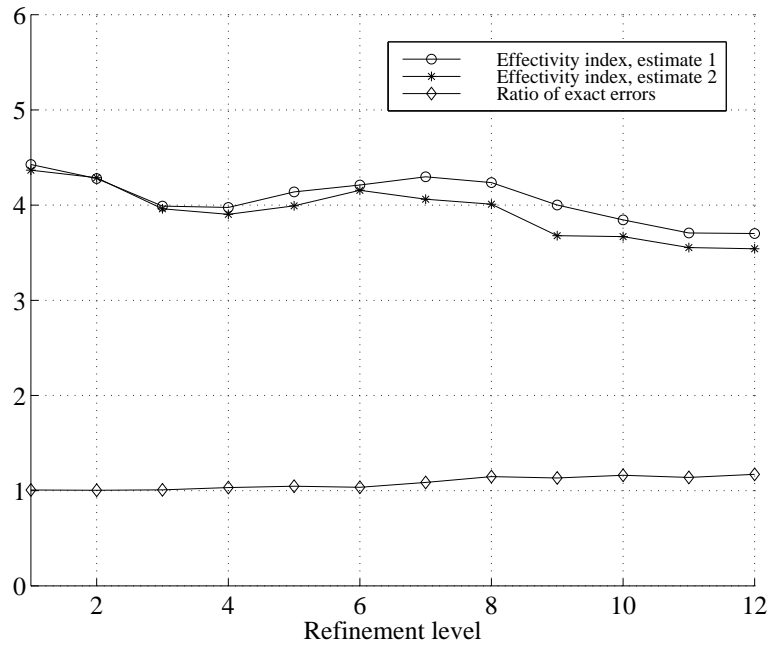
FIGURE 11. Elevation of the approximate solution.

FIGURE 12. Effectivity index obtained on a sequence of adaptively refined meshes.

REFERENCES

[1] R. Becker, P. Hansbo, and R. Stenberg, A finite element method for domain decomposition with non-matching grids, M2AN Math. Model. Numer. Anal., in press.

[2] M. J. Berger, On conservation at grid interfaces, *SIAM J. Numer. Anal.* 24 (1987) 967–984

[3] S.C. Brenner and L.R. Scott. *The Mathematical Theory of Finite Element Methods.* Springer-Verlag, Berlin, 1994

[4] F. Brezzi, J.-L. Lions, and O. Pironneau, Analysis of a Chimera method, *C. R. Math. Acad. Sci. Paris* 332 (2001) 655–660

[5] G. Chesshire and W. D. Henshaw, Composite overlapping meshes for the solution of partial-differential equations, *J. Comput. Phys.* 90 (1990) 1–64

[6] V. Girault, P.-A. Raviart, *Finite Element Approximation of the Navier-Stokes Equations*, Springer-Verlag, Berlin, 1979

[7] A. Hansbo and P. Hansbo, An unfitted finite element method, based on Nitsche's method, for elliptic interface problems, *Comput. Methods Appl. Mech. Engrg* 191 (2002) 5537–5552

[8] R. D. Lazarov, J. E. Pasciak, J. Schöberl, and P. S. Vassilevski, Almost optimal interior penalty discontinuous approximations of symmetric elliptic problems on non-matching grids, Preprint.

[9] R. D. Lazarov, S. Z. Tomov, and P. S. Vassilevski, Interior penalty discontinuous approximations of elliptic problems, *Comput. Methods Appl. Math.* 1 (2001) 367–382.

[10] J. Nitsche, Über ein Variationsprinzip zur Lösung von Dirichlet-Problemen bei Verwendung von Teilräumen, die keinen Randbedingungen unterworfen sind, *Abh. Math. Univ. Hamburg* 36 (1971) 9–15.

[11] L.R. Scott and S. Zhang, Finite element interpolation of nonsmooth functions satisfying boundary conditions, *Math. Comp.* 190 (1990) 483–493.

[12] R. Stenberg, Mortaring by a method of J.A. Nitsche. In *Computational Mechanics: New Trends and Applications,* S. Idelsohn, E. Onate and E. Dvorkin, Eds., CIMNE, Barcelona (1998).

CHALMERS FINITE ELEMENT CENTER PREPRINTS

2001–01 *A simple nonconforming bilinear element for the elasticity problem*
Peter Hansbo and Mats G. Larson

2001–02 *The $\mathcal{LL}^*$ finite element method and multigrid for the magnetostatic problem*
Rickard Bergström, Mats G. Larson, and Klas Samuelsson

2001–03 *The Fokker-Planck operator as an asymptotic limit in anisotropic media*
Mohammad Asadzadeh

2001–04 *A posteriori error estimation of functionals in elliptic problems: experiments*
Mats G. Larson and A. Jonas Niklasson

2001–05 *A note on energy conservation for Hamiltonian systems using continuous time finite elements*
Peter Hansbo

2001–06 *Stationary level set method for modelling sharp interfaces in groundwater flow*
Nahidh Sharif and Nils-Erik Wiberg

2001–07 *Integration methods for the calculation of the magnetostatic field due to coils*
Marzia Fontana

2001–08 *Adaptive finite element computation of 3D magnetostatic problems in potential formulation*
Marzia Fontana

2001–09 *Multi-adaptive galerkin methods for ODEs I: theory & algorithms*
Anders Logg

2001–10 *Multi-adaptive galerkin methods for ODEs II: applications*
Anders Logg

2001–11 *Energy norm a posteriori error estimation for discontinuous Galerkin methods*
Roland Becker, Peter Hansbo, and Mats G. Larson

2001–12 *Analysis of a family of discontinuous Galerkin methods for elliptic problems: the one dimensional case*
Mats G. Larson and A. Jonas Niklasson

2001–13 *Analysis of a nonsymmetric discontinuous Galerkin method for elliptic problems: stability and energy error estimates*
Mats G. Larson and A. Jonas Niklasson

2001–14 *A hybrid method for the wave equation*
Larisa Beilina, Klas Samuelsson and Krister Åhlander

2001–15 *A finite element method for domain decomposition with non-matching grids*
Roland Becker, Peter Hansbo and Rolf Stenberg

2001–16 *Application of stable FEM-FDTD hybrid to scattering problems*
Thomas Rylander and Anders Bondeson

2001–17 *Eddy current computations using adaptive grids and edge elements*
Y. Q. Liu, A. Bondeson, R. Bergström, C. Johnson, M. G. Larson, and K. Samuelsson

2001–18 *Adaptive finite element methods for incompressible fluid flow*
Johan Hoffman and Claes Johnson

2001–19 *Dynamic subgrid modeling for time dependent convection–diffusion–reaction equations with fractal solutions*
Johan Hoffman

2001–20   *Topics in adaptive computational methods for differential equations*
Claes Johnson, Johan Hoffman and Anders Logg

2001–21   *An unfitted finite element method for elliptic interface problems*
Anita Hansbo and Peter Hansbo

2001–22   *A P^2–continuous, P^1–discontinuous finite element method for the Mindlin-Reissner plate model*
Peter Hansbo and Mats G. Larson

2002–01   *Approximation of time derivatives for parabolic equations in Banach space: constant time steps*
Yubin Yan

2002–02   *Approximation of time derivatives for parabolic equations in Banach space: variable time steps*
Yubin Yan

2002–03   *Stability of explicit-implicit hybrid time-stepping schemes for Maxwell's equations*
Thomas Rylander and Anders Bondeson

2002–04   *A computational study of transition to turbulence in shear flow*
Johan Hoffman and Claes Johnson

2002–05   *Adaptive hybrid FEM/FDM methods for inverse scattering problems*
Larisa Beilina

2002–06   *DOLFIN - Dynamic Object oriented Library for FINite element computation*
Johan Hoffman and Anders Logg

2002–07   *Explicit time-stepping for stiff ODEs*
Kenneth Eriksson, Claes Johnson and Anders Logg

2002–08   *Adaptive finite element methods for turbulent flow*
Johan Hoffman

2002–09   *Adaptive multiscale computational modeling of complex incompressible fluid flow*
Johan Hoffman and Claes Johnson

2002–10   *Least-squares finite element method with applications in electromagnetics*
Rickard Bergström

2002–11   *Discontinuous/continuous least-squares finite element methods for Elliptic Problems*
Rickard Bergström and Mats G. Larson

2002–12   *Discontinuous least-squares finiteeElement methods for the Div-Curl problem*
Rickard Bergström and Mats G. Larson

2002–13   *Object oriented implementation of a general finite element code*
Rickard Bergström

2002-14   *On adaptive strategies and error control in fracture mechanics*
Per Heintz and Klas Samuelsson

2002-15   *A unified stabilized method for Stokes' and Darcy's equations*
Erik Burman and Peter Hansbo

2002-16   *A finite element method on composite grids based on Nitsche's method*
Anita Hansbo, Peter Hansbo and Mats G. Larson

These preprints can be obtained from

www.phi.chalmers.se/preprints